RSC Applied Polymers

ROYAL SOCIETY OF CHEMISTRY

COMMUNICATION

View Article Online
View Journal | View Issue

Check for updates

Cite this: *RSC Appl. Polym.*, 2024, **2**, 606

Received 25th March 2024,
Accepted 15th April 2024

DOI: 10.1039/d4lp00109e

rsc.li/rscapplpolym

Branched benzocyclobutene polysiloxane with excellent photo-patterning and low dielectric properties†

Juan Peng,[a] Chao Guo,[a] Xinyu Hu,[a] Hanlin Du,[a] Qiuxia Peng,[b] Huan Hu,[c] Wentao Yuan,[a] Junxiao Yang *[a] and Jiajun Ma *[a]

The photoresist is one of the key materials for the development of the modern semiconductor industry, and it not only affects the chip manufacturing process but also has an important impact on performance. Photoresists with low dielectric properties have a critical impact on the fabrication process and performance of various chips and devices. In this paper, a silicone encapsulated photoresist with low dielectric properties is reported, and it demonstrates excellent film-forming properties and lithography patterning effects, with a line width of 10 μm and a line spacing, a low dielectric constant (D_k = 2.75), a high thermal decomposition temperature (T_5 = 503.5 °C), a low coefficient of thermal expansion (CTE = 33.61 ppm per °C), and excellent mechanical properties of thin films. This type of resin has a photo-crosslinked double bond structure and a thermally cross-linked benzocyclobutene structure, in which the silicone branched structure gives the photoresist excellent patterning properties and the thermally crosslinked structure gives the film excellent thermal, electrical, and mechanical properties. The resin is expected to replace traditional polyimide photoresists and has important applications in the semiconductor industry.

Lithography is crucial for manufacturing integrated circuits. It utilizes photochemical reactions and physical etching on a chip for precise pattern transfer.[1–3] The photoresist is a key material in lithography technology, and has undergone several iterations, from polyvinyl ethyl cinnamate to epoxy and various acrylic resins.[4–7] The application of epoxy resin and acrylic resin in photoresists is limited. Polysiloxane is a better alternative due to its excellent thermal and electrical properties. UV curing technology helps to develop polysiloxanes. Hyperbranched polysiloxanes have better fluidity, solubility, and lower viscosity than linear polysiloxanes.[8] A hyperbranched polysiloxane resin has abundant silicon–oxygen bonds, making it flexible and reducing intermolecular forces. It has a low glass transition temperature, surface tension, energy, solubility, and dielectric constant. UV curing technology has become an ideal choice due to its advantages such as fast curing, low pollution, low energy consumption, and good chemical stability.[9–12] Therefore, the combination of the two makes it have broad application prospects in the field of UV curing.[13–15] Kirchhoff[16] synthesized DVSBCB through the Heck reaction. Dow Chemical obtained the DVSBCB resin through thermal polymerization and created light-curable photoresists by changing the photoinitiator and solvent conditions.

Microelectronics requires miniaturization and high integration of electronic devices, resulting in increased wiring density in integrated circuits, as well as increased resistance capacitance and power consumption between metal resistors and wire layers due to reduced feature sizes.[17–22] The use of low dielectric constant materials is an effective way to solve this problem. The low dielectric constant and the loss of interlayer dielectric materials can improve the propagation speed and loss of signals at high frequencies.[23–25] The benzocyclobutene (BCB) resin is very popular in this regard. A team developed vinyl silane monomers that connect BCB groups to silicon atoms, forming polybenzocyclobutene silane with vinyl side chains and excellent electrical properties. BCB groups were introduced into vinyl-containing POSS to create star-type multi-arm BCB-functionalized POSS compounds with good low dielectric properties.[26] Double bonds were retained after adding 4-alkynyl benzocyclobutene to the cage-like structure, which is suitable for lithographic patterning.[27] BCB was combined with the flexibility of the Si–O bond structure to make a linear, low-dielectric benzocyclobutenylsiloxane material.[28,29] Double bonds in the polysiloxane structure provide a structural basis for lithographic patterning.

The paper presents a branched benzocyclobutene polysiloxane resin (HBPSi-1, HBPSi-2, and HBPSi-3) with double bonds and BCB groups (Fig. 1(A)). It has good thermal properties and can create complex patterns with good resolution through UV

[a]*School of Materials and Chemistry and State Key Laboratory of Environmentally-friendly Energy Materials, Southwest University of Science and Technology, Mianyang 621010, China. E-mail: yangjunxiao@swust.edu.cn, jiajunma@yeah.net*
[b]*School of Materials Science and Engineering, Sichuan University of Science & Engineering, Zigong 643000, China*
[c]*Tiannuo Photoelectric Material Co., Ltd, Ji'nan, 250000, China*
† Electronic supplementary information (ESI) available. See DOI: https://doi.org/10.1039/d4lp00109e

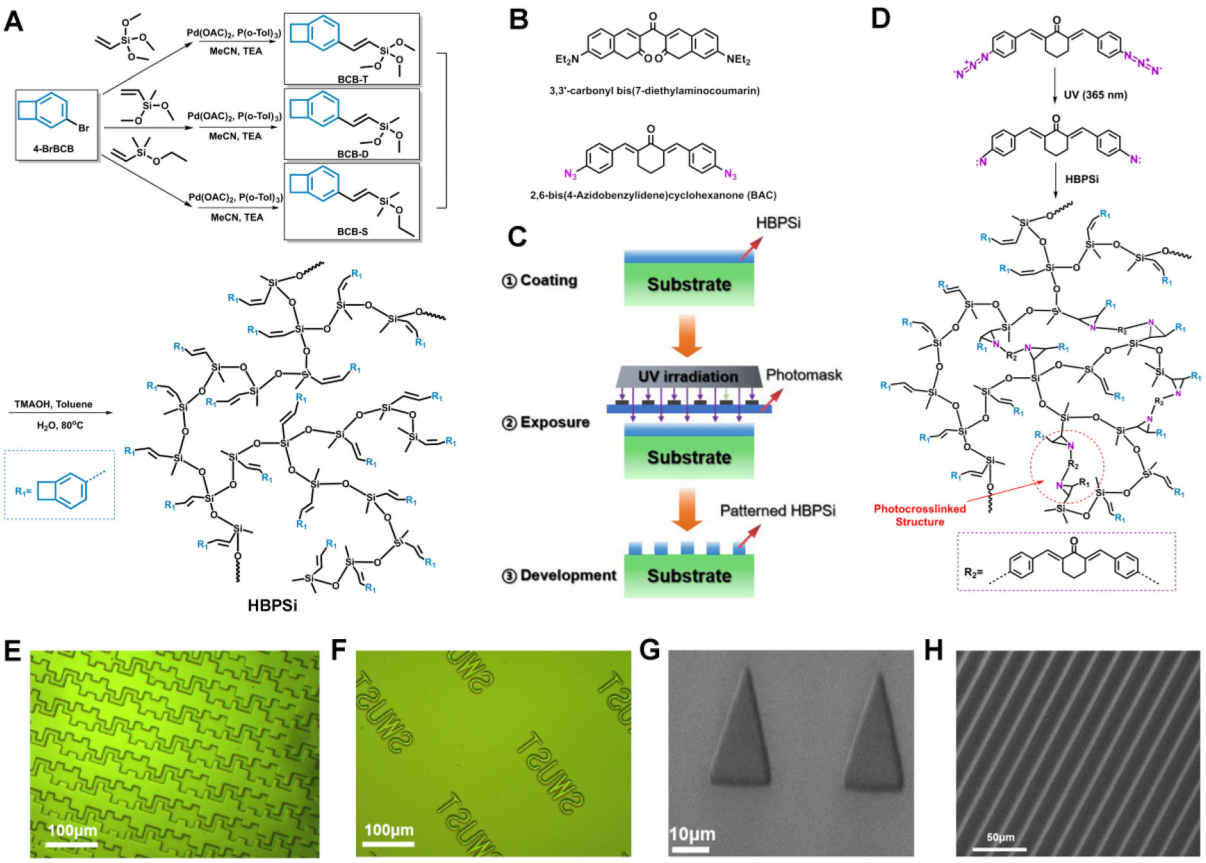

Fig. 1 (A) The synthesis route of the branched polymer; (B) chemical structures of photoinitiators; (C) lithography patterning process; (D) photocuring mechanism of branched resins; (E and F) lithography patterning under an optical microscope; (G and H) photolithography patterning under SEM.

curing. The resin has excellent electrical, mechanical, and thermal properties and undergoes photocrosslinking during the photolithography process with azide photoinitiators under UV light.

Three functionalized BCB monomers were synthesized by the Heck reaction, and branched polysiloxane resins with different ratios were prepared through hydrolysis condensation. ^{1}H NMR and ^{13}C NMR were used to characterize the structure of the resins, and detailed steps are provided in the ESI (Fig. S1 and S2†). By adding a photoinitiator, photosensitizer, and solvent to the resin, a complex pattern with a minimum line width and line spacing of 10 μm was obtained by UV curing (Fig. 1 (E-H)), with clear edges, no adhesion, no photoresist residue. The DLS particle size of the resin was tested (Table S2†). The test results showed that the average particle size of the resin was 484.78 nm, the crosslinking effect was good, and there were no large gel particles and residues after development. A rough analysis was conducted on the mechanism of UV curing (Fig. 1(D)), where 3,3-carbonyl bis(7-diethylamino coumarin) absorbs photons that transition from the ground state to the excited singles triplet excited state of 3,3-carbonyl bis(7-diethylamino coumarin) reacts with 2,6-bis (4-azophenylmethylene)cyclohexanone to form carbonyl and amine radicals, which react with double bonds in the polymer resin to form a nitrogen-doped ternary ring.2,6-Bis(4-azophenylmethylene)cyclohexanone generates nitrogen carbene, which undergoes photocrosslinking reaction with the double bond in the polymer resin to form a nitrogen-doped ternary ring.

The triplet excited state of 3,3-carbonyl bis(7-diethylaminocoumarin) reacts with 2,6-bis(4-azophenylmethylene) cyclohexanone to form carbonyl and amine radicals, which react with double bonds in the polymer resin to form a nitrogen-doped ternary ring.

Fourier transform infrared spectroscopy was used to study the UV curing kinetics of photosensitive resins. The absorption peak of azide at 2100 cm^{-1} gradually decreased with the increase of illumination time, and the characteristic absorption peak of vinyl at 980 cm^{-1} in the resin gradually decreased (Fig. 2(A)). Still, the change was not significant, which confirmed the photocrosslinking reaction of double bonds under ultraviolet light. Fig. 2(B) shows the changes in azide and double bonds at different UV curing times with integration of the absorption peaks of azide and double bonds in the FT-IR spectrum of UV curing kinetics. We can objectively understand that with the increase of curing time, the azide compound undergoes a chemical reaction and generates nitrogen carbene radicals, which react with the double bond to form a nitrogen ternary ring, increase the degree of resin cross-linking, and produce a good lithography pattern.

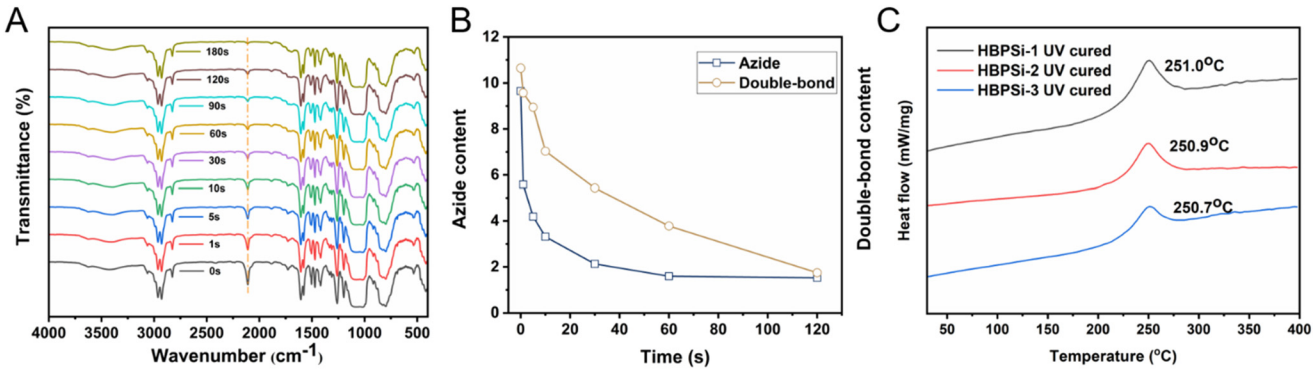

Fig. 2 (A) Infrared spectra of azide content and double bond content at different UV illumination times; (B) the change of azide and double bond content with illumination time; (C) DSC curves of the resins after photocuring.

Therefore, the azide compound will gradually weaken with the curing time, showing a trend of first fast and then slow weakening, and the change of the double bond has a lag compared with it.

The UV curing behavior of three branched benzocyclobutene polysiloxane photosensitive resins with different proportions is shown in Fig. 2(C). The photosensitive resin has a curing exothermic peak with an initial temperature of 225 °C and a curing exothermic peak at 250 °C, indicating the reaction peak after BCB ring opening. The final temperature is 275 °C, and the subsequent curve is smooth, indicating that the ring-opening reaction is basically over and the photosensitive resin is completely cured.

The properties of photothermally cured and pure thermocured resins were studied and compared. The curing behavior of the three kinds of branched polysiloxane resins was studied by differential calorimetry (DSC). In a N_2 atmosphere, the room temperature rises to 400 °C and the heating rate is 10 °C per min. It is not difficult to see that the three resins show similar exothermic behavior, there is no obvious exothermic peak in the cured resins, and the curve is flat, which indicates that all the resins have been cured completely under the set curing conditions (Fig. S4†).

The variation of functional groups under different curing states is shown in Fig. S3.† The change of the absorption peak at 2840 cm^{-1} may be caused by the vibration after carbon–hydrogen hexacyclization after heat curing, and the characteristic absorption peak of the C=C bond of olefin at 1610 cm^{-1} has a weakening trend after light curing, indicating that a small number of double bonds are cross-linked during light curing, and the characteristic absorption peak decreases sharply after heat curing, and most of the double bonds in the resin are thermally cross-linked. The results showed that the vinyl double bond underwent a two-step curing, first photocross-linked and then heat-cross-linked, and a Diels Alder reaction with the active *o*-quinoline methane occurred.

The thermal stability of the branched resin was studied by thermogravimetric analysis (TGA). According to the TGA curve, the 5% weight loss temperature ($T_{5\%}$) and the maximum thermal decomposition rate of the heat-curing resin was determined, and the stability of the three medium-branched resins was ranked, as shown in Fig. 3(A): HBPSi-1 > HBPSi-3 > HBPSi-2; with the increase of BCB groups and the increase of the cross-linking degree, the thermal stability is also significantly improved, but HBPSi-2, as a special case, does not follow the law of its development. It is speculated that the possible reason is that the cross-linking degree of the polymer in the hydrolysis process is not up to the ideal situation, resulting in poor thermal stability. The HBPSi-1 resin has a high degree of crosslinking, so its thermal stability is high. Fig. 3(B) shows the TGA curve of the photo-heat-cured resin, whose thermal stability follows the order HBPSi-1 > HBPSi-2 > HBPSi-3; the reason for this may be that the photosensitizer leads to cross-linking within and between its molecules, which improves the degree of cross-linking. However, the addition of the photosensitizer affects the structural densification of the resin during the curing process, resulting in the weakening of thermal stability. These branched resins have a large number of Si–O–Si bonds as the main inorganic skeleton structure, and their high bond energy brings high stability. The six-membered or eight-membered ring structure formed by the ring opening of BCB after thermal curing forms a large planar structure with the benzene ring of the BCB body, which also has high stability. These two factors can ensure that these resins are not thermally decomposed at 460 °C and have high thermal stability.

As shown in Fig. S5,† the DTG curve of the cured resin shows a single peak for both the heat-cured resin and the light-cured resin. Based on the DTG graph, the temperature corresponding to the maximum decomposition rate of the cured resin can be calculated. The maximum decomposition rate of all cured resins is above 500 °C, indicating that these cured resins have high thermal stability and can meet the performance requirements of packaging materials.

The linear coefficient of thermal expansion (CTE) of the branched resins with three different proportions when the room temperature rises to 300 °C (10 °C per min) in a N_2 atmosphere is shown in Fig. 3(G). The coefficient of thermal expansion reflects the degree of cross-linking of the resin material, and a higher degree of cross-linking at high temperatures will hinder the free movement of the molecular segments, making

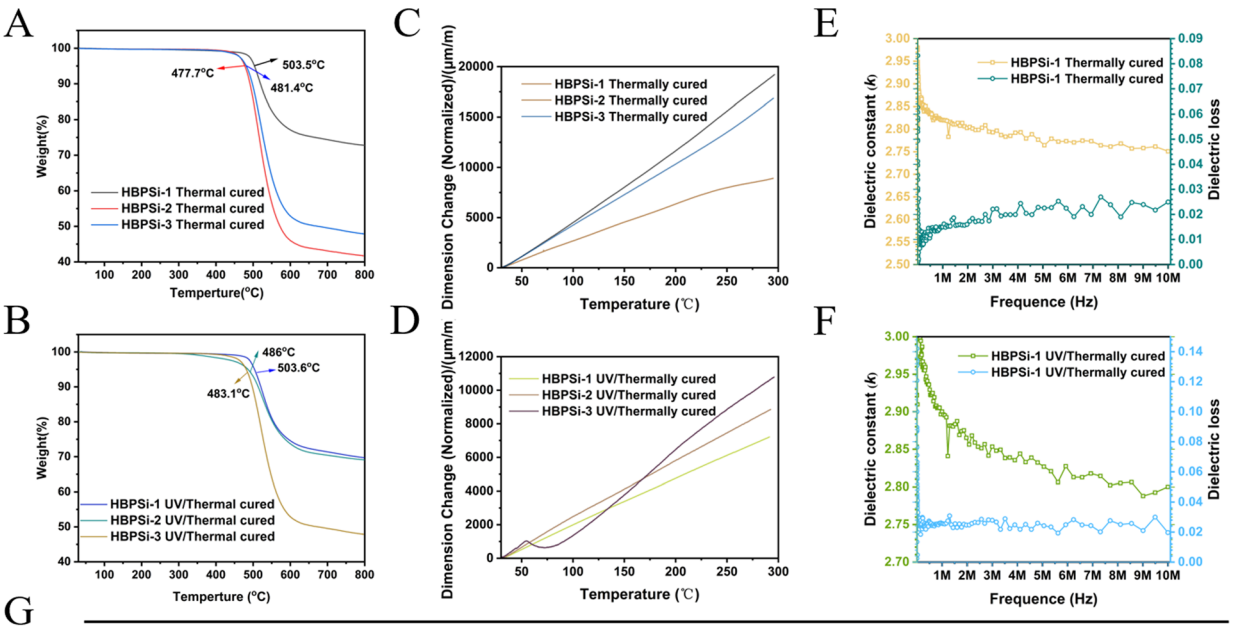

G

Sample	$T_{5\%}$ (°C)	Temperature for maximum decomposition rate	CTE[a] (ppm/°C)	Elastic modulus (Gpa)	Hardness (Gpa)	k
Cured HBPSi-1	503.5	516	33.61	6.2	0.53	2.75
CuredHBPSi-2	477.7	503	72.13	4.5	0.43	-
Cured HBPSi-3	481.4	507	63.46	5.17	0.48	-
UV/T cured HBPSi-1	503.6	506	27.68	7.4	0.73	2.80
UV/T cured HBPSi-2	486.0	512	33.88	6.6	0.55	-
UV/T cured HBPSi-3	483.1	511	45.89	6.1	0.53	-
RC-T/PMAPS [30]	402.0	-	-	-	-	2.30
BMSs [31]	495.0	-	51.57	3.7	0.24	2.77
DVSBCB [32]	440.7	-	47.0±3.0	-	-	2.65

Fig. 3 (A, C, and E) TG, TMA, and dielectric constants of heat-cured resins; (B, D, and F) TG, TMA, and dielectric constants of the photothermally cured resins; (G) comparison of the properties of resins[30–32].

the material structure more stable. Fig. 3(C) shows the CTE curve of the heat-cured resin.

The results show that with the increase in temperature, the curve is relatively smooth, indicating that the thermal stability of the resin after curing is good in this temperature range, and the distribution of the cured resin system is relatively uniform. HBPSi-1 has the lowest CTE of the three resins (33.61 ppm per °C). The reason is that with the increase of BCB groups, the cross-linking network structure generated by open-loop cross-linking becomes more dense, and the deformation decreases at a high cross-linking degree. The CTE results of the HBPSi-2 resin were the highest, which confirmed that the degree of hydrolysis was not high, the degree of intermolecular cross-linking was insufficient, and the free movement of molecular chains was enhanced.

Fig. 3(D) shows the CTE curve of the photothermally cured resin. The results show that with the increase of crosslinking, the volume of CTE becomes smaller and the thermal expansion performance is excellent. Comparing the CTE of heat-cured resins with photo-heat-cured resins, it can be seen that the CTEs of photo-heat-cured resins are lower than those of heat-cured resins.

The results showed that with the increase of the cross-linking degree, the thermal stability of the photosensitive resin became better, and was significantly better than that of the commercially available DVSBCB ($T_{5\%}$ = 440.7 °C) resin.

The mechanical properties of the three kinds of branched benzocyclobutene polysiloxane resins with different proportions after curing were tested by the nanoindentation method. The results of the mechanical properties of the heat-cured resins are shown in Fig. 4. It shows that the higher the degree of branching, the higher the elastic modulus and hardness of the heat-cured resins, with the trend of a gradual increase. The reason for this phenomenon may be that the higher the degree of branching, the higher the cross-linking degree of the resin in the process of heat-curing, and the higher the elastic modulus and hardness. The average modulus and hardness of the heat-cured resin are between 4.5–7.4 Gpa and 0.43–0.73 Gpa, respectively. Among them, the HBPSi-1 heat-cured resin has the highest elastic modulus (7.4 Gpa) and hardness (0.73 Gpa), which is attributed to the presence of more BCB groups in the heat-cured structure with a higher crosslinking degree.

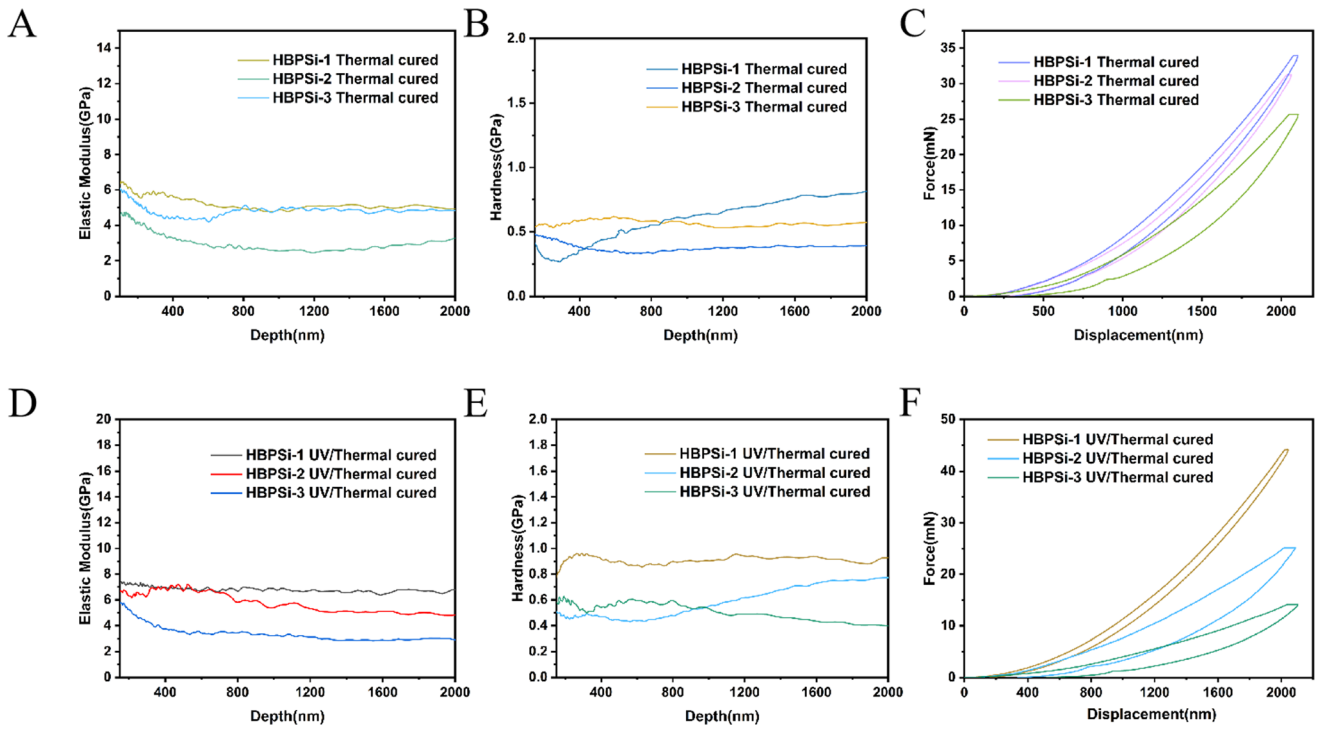

Fig. 4 (A, B, and C) Modulus, hardness, and load–unload curves of the thermocured resins; (D, E, and F) modulus, hardness, and load–unload curves of the photothermally cured resins.

The test results of the photothermally cured resins are shown in Fig. 3(G). From Fig. 4, it can be concluded that the mechanical properties of the three photosensitive resins with different proportions are ranked as HBPSi-1 > HBPSi-2 > HBPSi-3; the reason for this result may be that some double bonds cross-linked during the photocuring process, and thermal curing further strengthened the cross-linking effect of curable groups, resulting in more curable cross-linked groups and the better mechanical properties of the cured resin surface.

The electrical properties of the cured resin were measured at a frequency of 10 MHz and the results are shown in Fig. 3 (G). Fig. 3(E) and (F) show the thermal curing of the HBPSi-1 resin measured at 10 MHz and the change in dielectric constant after photothermal curing. The dielectric constant is relatively stable in this frequency range. Under these conditions, the dielectric constant (D_k) of the heat-cured HBPSi-1 resin was 2.75 at 10 MHz, and the dielectric constant (D_k) of the photothermally cured resin was 2.80, indicating that the dendritic benzocyclobutyl polysiloxane resin has good low dielectric properties. It meets the requirements for low dielectric properties, but the photosensitizer residue results in a high dielectric constant of the photothermally cured resin. The resin is dominated by the special skeleton structure of Si–O–Si, and the cyclic structure of the benzo-six-membered ring is formed after BCB heat curing, and the existence of a large number of cavities effectively reduces the dielectric constant of the resin.

The hydrophobicity of the cured resin film was determined by measuring the contact angle of water droplets on the film in a static environment. As shown in Fig. S7(A and B),† the contact angles of HBPSi-1, HBPSi-2, and HBPSi-3 thermosetting resin films are 102°, 96°, and 106°, respectively, and the contact angles of photothermally cured branched benzocyclobutene polysiloxane resin films are 101°, 106°, and 107°, respectively. This indicates that the resin films prepared by the two curing methods have good hydrophobicity.

Branched benzocyclobutene polysiloxane resins are prepared by hydrolysis and condensation, and they contain a large number of vinyl double bond groups, which provide the possibility of UV curing and forming visible films with complex patterns. Scanning electron microscopy (SEM) and optical microscopy (OPM) analysis showed that the material has good image-making properties. The structures of monomers and polysiloxane resins were characterized by infrared spectroscopy, nuclear magnetic hydrogen spectroscopy, and carbon spectroscopy. The results showed that the monomer and resin were successfully prepared. The presence of different hydrolyzable functional groups ensures the smooth preparation of branched resins. The BCB-S capping agent reduces the presence of Si-OH, while the cured BCB group rings open to form a new ring structure and the inorganic Si–O–Si structure ensures low dielectric properties. The heat-cured branched benzocyclobutene polysiloxane resin has good mechanical properties, excellent thermal properties and dielectric properties due to the cross-linking reaction that

occurs to form a benzo six-membered ring by opening the benzo quaternary ring during the curing process to form a dense structure. Compared with thermally cured and photo-thermally cured resins, photosensitive resins have good mechanical, thermal and dielectric properties, and hence have good application prospects in the field of encapsulated photoresists.

Author contributions

Juan Peng, Jiajun Ma, and Junxiao Yang designed and engineered the samples; Juan Peng and Chao Guo performed the experiments; Juan Peng, Xinyu Hu, Hanlin Du, and Wentao Yuan assisted with the sample testing; Juan Peng, Qiuxia Peng, Huan Hu, Jiajun Ma and Junxiao Yang helped with manuscript writing. All authors contributed to the general discussion.

Conflicts of interest

There are no conflicts to declare.

Acknowledgements

This work was financially supported by the Sichuan Science and Technology Program (no. 2022NSFSC0032 and no. 24NSFSC1595) and the Open Fund of State Key Laboratory of Environment-Friendly Energy Materials, Southwest University of Science and Technology (no. 21fksy03 and no. 20fksy03).

References

1 X. K. Peng, X. W. Huang, R. T. Liu, *et al.*, *Chin. J. Appl. Chem.*, 2021, **38**(9), 1079–1090.
2 H. Wu, Y. Wang, J. Yu, J.-A. Pan, H. Cho, *et al.*, *J. Am. Chem. Soc.*, 2022, **144**, 10495–10506.
3 Y. Wang, L. Fedin, H. Zhang and D. V. Talanin, *Science*, 2017, **357**, 385–388.
4 S. Murase, K. Kinoshita, K. Hoorie, *et al.*, *Macromolecules*, 1997, **30**(25), 8088–8090.
5 J. V. Crivello and J. L. Lee, *J. Polym. Sci., Part A: Polym. Chem.*, 1990, **28**(3), 47.
6 A. L. Bogdanov, V. A. Nikitaev and A. A. Polyakov, *Proc. SPIE*, 1990, **1262**, 425–431.
7 C. Özeroğlu and N. Metin, *J. Radioanal. Nucl. Chem.*, 2012, **292**(2), 923–935.
8 E. Yilgör and I. Yilgör, *Prog. Polym. Sci.*, 2014, **39**(6), 1165–1195.
9 P. Mohan, *Polym.-Plast. Technol. Eng.*, 2013, **52**(2), 107–125.
10 J. Qin, H. Zhao, Z. Qin, *et al.*, *Polym. Compos.*, 2021, **42**(7), 3445–3457.
11 A. Shimojima and K. Kuroda, *Molecules*, 2020, **25**(3), 524.
12 X. Han, X. Zhang, Y. Guo, *et al.*, *Polymers*, 2021, **13**(9), 1363.
13 M. E. Mills, P. Townsend, D. Casillo, *et al.*, *Microelectron. Eng.*, 1997, **33**(1–4), 327–334.
14 J. S. Rathore and L. V. Interrante, *Macromolecules*, 2009, **42**(13), 4614–4621.
15 Y. Jung, T. H. Yeo, W. Yang, *et al.*, *J. Phys. Chem. C*, 2011, **115**(50), 25056–25062.
16 R. A. Kirchhoff and K. J. Bruza, *Prog. Polym. Sci.*, 1993, **18**, 85–185.
17 H. Xu, V. Kosma, E. P. Giannelis, *et al.*, *Polym. J.*, 2018, **50**(1), 45–55.
18 C. C. Chiu, C. C. Lee, T. L. Chou, C. C. Hsia and K. N. Chiang, *Microelectron. Eng.*, 2008, **85**, 2150–2154.
19 T. Song, W. Rim, S. Park, *et al.*, *IEEE J. Solid-State Circuits*, 2016, **52**(1), 240–249.
20 R. Li, X. Yang, J. Li, *et al.*, *Mater. Today Phys.*, 2022, **22**, 100594–100612.
21 M. A. Wolfgang, *Curr. Opin. Solid State Mater. Sci.*, 2002, **6**(5), 371–377.
22 M. Xie, M. Li, Q. Sun, *et al.*, *Mater. Sci. Semicond. Process.*, 2022, **139**, 106320–106333.
23 R. Bowrothu, H.-L. Kim, C. S. Smith, *et al.*, *IEEE Trans. Microw. Theory Techn.*, 2020, **68**(12), 5065–5071.
24 W. Hu, Z. Chen, L. Qian, *et al.*, *IEEE Trans. Antennas Propag.*, 2022, **70**(7), 5254–5265.
25 M. Nabil and M. M. A. Faisal, *Wirel. Pers. Commun.*, 2020, **116**, 2761–2776.
26 X. B. Zuo, X. J. Zhao, B. Liu, *et al.*, *J. Appl. Polym. Sci.*, 2009, **112**, 2781–2791.
27 C. O. Hayes, B. K. Mueller, W. K. B. Philip Liu, *et al.*, *J. Ceram. Soc. Jpn.*, 2015, **123**(1441), P9-1–P9-3.
28 Q. X. Peng, H. Hu, Y. t. Deng, *et al.*, *J. Mater. Chem. C*, 2022, **10**, 9106.
29 Q. Peng, J. Ma, J. Wu, *et al.*, *Polym. Chem.*, 2023, **14**, 3446–3452.
30 S. Chen, D. Zhuo and J. Hu, *Ind. Eng. Chem. Res.*, 2018, **57**(31), 10372–10378.
31 H. Wei, X. Li, *et al.*, *Polymers*, 2023, **15**(13), 2843.
32 G. Huang, L. Fang, *et al.*, *Polym. Chem.*, 2021, **12**, 402–407.